Solar Energy 263 (2023) 111816

Contents lists available at ScienceDirect

Solar Energy

journal homepage: www.elsevier.com/locate/solener

Simulation and economic analysis of an innovative indoor solar cooking system with energy storage

Chang Zhou [a,b], Yinfeng Wang [a,*], Jing Li [b], Xiaoli Ma [b,*], Qiyuan Li [c], Moucun Yang [a], Xudong Zhao [b], Yuezhao Zhu [a]

[a] School of Energy Science and Engineering, Nanjing Tech University, 30 Puzhu South Rd., Nanjing 211816, China
[b] Centre for Sustainable Energy Technologies, University of Hull, Hull HU6 7RX, United Kingdom
[c] School of Mechanical and Manufacturing Engineering, The University of New South Wales, Kensington, New South Wales 2052, Australia

ARTICLE INFO

Keywords:
Solar cooking system
System performance
Configuration optimization
Economy

ABSTRACT

Solar energy technology and energy storage technology are promising to make a contribution to current energy and global climate issue. The energy demand of daily cooking is enormous, and conventional cooking methods use gas or electricity with large carbon emissions. This paper proposes an innovative solar cooking system (SCS) integrated with rock-bed thermocline storage. Thermal oils transfer heat from the collectors to the rocks in the charging process and release heat in cooktop unit for cooking. The energy consumption of a household is first assessed by a reasonable hypothesis. Mathematical models and simulation models are then established to analyze the heat transfer performance of the cooktop unit and the annual running performance of the SCS. The rock-bed thermocline storage, single-tank thermocline storage and two-tank storage are compared. The simulation results indicate that the rock-bed thermocline storage unit employed to SCS will enhance the annual running performance and acquire the minimum initial investment cost. The economic analysis shows that the lowest levelized cost of cooking energy (LCOC) of the SCS is 0.3884 $/kWh, while the corresponding levelized cost of cooking a meal (LCCM) is 0.953 $/Meal and the solar fraction (SF) is 71%. Compared to the electrical and natural gas cooker, the SCS saves 1.75 tons and 0.52 tons of carbon emissions annually, respectively.

1. Introduction

Residential energy consumption is the third largest sector of global total energy consumption [1], especially in many developing countries, with cooking accounting for most household energy consumption [2]. At present, the main types of cooking energy are LPG, natural gas, electricity and biomass energy. In the context of the goal of achieving net zero emissions in the future proposed by countries worldwide, more advanced thermal utilization technologies which use clean, renewable energy need to be promoted to meet this development goal and alleviate the consumption and dependence on traditional energy. As of now, solar energy technology and thermal energy storage (TES) technology remain a hot topic for future research in the development of new energy technology which has been gradually popularized and used in various fields, such as solar power plants, solar auxiliary heating and cooling for buildings, etc [3]. Due to the solar collector and TES technologies getting more mature and cost-effective, using solar energy for cooking is a well application, the medium-temperature (80–250 °C) thermal energy is generated by the collector and stored by the TES unit (150–200 °C). Many research achievements have been made in the field of solar cookers, and all kinds of solar cookers and cooking systems have been proposed.

In general, solar cookers can be classified into three types, that are box type, concentrating type and indirect solar cooker [4]. R. M. Muthusivagami et al. [5] classified solar cookers in the literature review, as shown in Fig. 1. Mohamad Aramesh et al. [6] reviewed the last 20 years of research on improving solar cookers, and it is obvious that many researchers have conducted many studies on direct solar cookers, especially box type solar cookers. Cuce et al. [7] improved the traditional box type solar cooker by adding a natural Bayburt stone for thermal energy storage. This design enabled the cooker to maintain a relatively higher operating temperature toward sunset, and enhanced the energy efficiency to 21.7–35.3%. Nevertheless, the conventional box type cookers of low operating temperature (up to about 100 °C) is difficult to meet most cooking requirements, especially in the short cooking time and the large cooking load. Tawfik et al. [8] further developed a box type solar cooker by introducing a tracking-type bottom

* Corresponding authors.
E-mail addresses: wangyf@njtech.edu.cn (Y. Wang), X.Ma@hull.ac.uk (X. Ma).

https://doi.org/10.1016/j.solener.2023.111816
Received 7 December 2022; Received in revised form 26 April 2023; Accepted 22 June 2023
Available online 20 July 2023

Nomenclature

A	Aperture area of solar collector (m^2)
a_1	First order loss coefficient (W/m^2-K)
a_2	Second order loss coefficient (W^2/m^4-K^2)
C_p	Specific heat capacity of heat transfer fluid (kJ/kg-K)
C_{po}	Specific heat capacity of oil (kJ/kg-K)
C_{p_R}	Specific heat capacity of rock (kJ/kg-K)
E	Input solar energy (kJ)
E_C	Energy input to cooktop (kJ)
$E_{C,a}$	Total input energy to cooktop annually (kJ)
$E_{C,e}$	Effective energy in cooking (kJ)
E_S	Energy stored in storage unit (kJ)
$E_{S,d}$	Designed value of energy stored in storage unit (kJ)
E_{SC}	Energy received by solar collector (kJ)
h_f	Convective heat transfer coefficient of the fluid inside the tank (W/m^2-K)
$1/h_{fo}$	Convective heat transfer resistance of the medium which is between the fluid and the tank wall (m^2-K/W)
h_o	Convective heat transfer coefficient of the air outside the tank (W/m^2-K)
I_b	Solar beam radiation (W/m^2)
i	Ordinal number of nodes
k_{ins}	Heat conductivity coefficient of insulation (W/m-K)
k_T	Heat conductivity coefficient of tank wall (W/m-K)
M	Mass of fluid (kg)
M_l	Annual cooking meals amount (Meal)
$\dot{m}_C$	Mass flow rate in the cooktop (kg/s)
$\dot{m}_{SC}$	Mass flow rate in the solar collector (kg/s)
$\dot{Q}_C$	Power of cooktop (kW)
$\dot{Q}_{SC}$	Power of solar collector (kW)
R	Total resistance of heat transfer (m^2-K/W)
T^*	Normalized temperature difference (m^2-K/W)
T_C	Temperature of cold fluid (°C)
T_H	Temperature of hot fluid (°C)
δ_{ins}	Thickness of insulation materials (mm)
δ_T	Thickness of storage tank wall (mm)
ε	Rock-bed void fraction (%)
η	Efficiency (%)
$t_{C,in}$	Temperature of the cooktop inlet (°C)
$t_{C,out}$	Temperature of the cooktop outlet (°C)
ρ_0	Density of heat transfer fluid (kg/m^3)
ρ_R	Density of the rock (kg/m^3)
τ	Cooking duration (s)

Subscripts

C	Cooktop unit
S	Storage unit
S,c	Storage unit charging
th	Thermal

Abbreviations

CC	Capital cost
CO_2	Carbon dioxide
CRF	Capital recovery factor
HLC	Heat loss coefficient
HTF	Heat transfer fluid
IAM	Incident angle modifier
kWh	Kilowatt-hour
LCCM	Levelized cost of cooking a meal
LCOC	Levelized cost of cooking energy
LCOE	Levelized cost of electricity
LPG	Liquefied petroleum gas
MPTC	Micro parabolic trough collector
MWh	Megawatt-hour
PCM	Phase change material
SCS	Solar cooking system
SF	Solar fraction
SMC	System maintenance cost
TES	Thermal energy storage
TSD	Thermal storage days

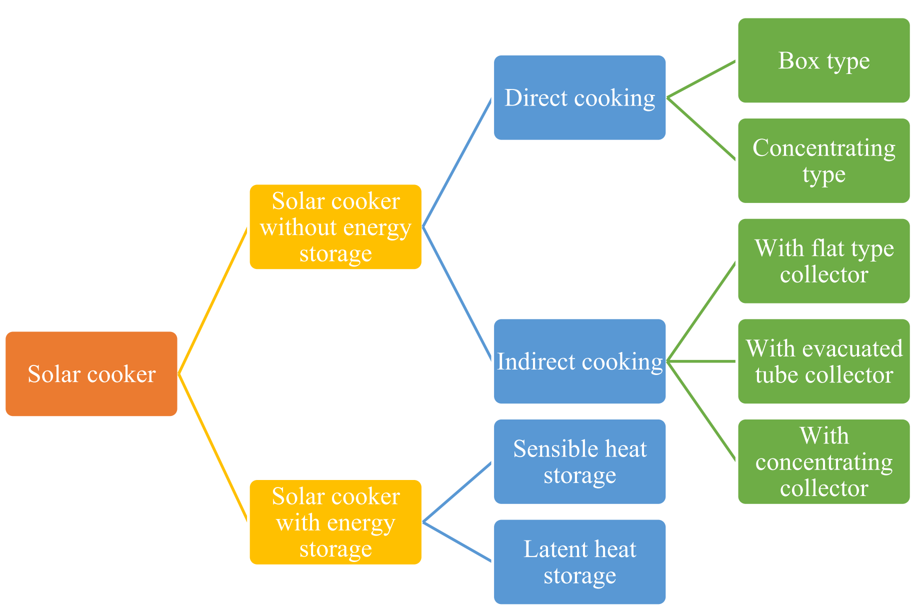

Fig. 1. Classification of solar cookers [5].

parabolic reflector, which could further improve the cooker temperature to 140 °C and shrink cooking time from 106 min to 83 min. Therefore, concentrating type solar cookers that generate higher temperatures are desired. Apaolaza-Pagoaga et al [9] developed a funnel cooker can reach operating temperature of 140 to 150 °C, while Ruivo et al. [10] achieved 180 °C. Sagade et al. [11] studied a parabolic dish solar cooker which has maximum temperature of 192.9 °C. Zhao et al. [12] developed a curved Fresnel lens solar cooker, which could operate at 361 °C. Bhave et al. [13] designed a dismountable cooking vessel filled of solar salt as the thermal energy storage medium. This kind of cooker could be taken into the kitchen for cooking when needed, which could reach 170–180 °C operating temperature. In the same way for cooking, Mawire et al. [14,15] compared sunflower oil and a PCM containing erythritol, respectively, as heat storage materials. The sunflower oil cooking pot shows a shorter cooking time (1.8–5.6 h) but attains a higher storage temperature (124–145 °C) and higher storage efficiency (3.0%-7.1%). On the contrary, the erythritol PCM pot has a longer cooking time (3.8–6.6 h), lower storage temperature (118–140 °C), and lower storage efficiency (2.5%-3.7%). However, direct solar cookers have the potential risk of heat discomfort and eye damage, due to the long time exposed outside and reflective concentrator use.

By contrast, indirect solar cookers may be more convenient for indoor cooking, and it is still the most promising type of solar cooker compared to direct solar cookers. Their biggest difference is whether there is a fluid medium involved in the heat transfer during the cooking process [5,6]. In indirect solar cookers, the fluid medium absorbs heat from the outdoor solar collector, transfers indoors, and releases it in the cooking pot (unit). In a real application of SCS from Kanyowa et al. [16] study, the system was used to produce steam of 150–170 °C temperature for indoor cooking pots. And 28 dish reflectors of 10 m^2 were installed on the rooftop, which could serve 6000 meals per day and enabled it to work around 200 days annually. O. K. Singh [17] studied an SCS, which consisted of a parabolic dish collector, a thermal oil T55 container, and a heat plate (cooking unit). The heat plate enables heating an existing pan directly for cooking, which could reach the highest temperature of 109 °C. Hosseinzadeh et al. [18,19] designed a cooking vessel along with the helical coil as a cooking unit which the thermal oil and oil-based nanofluids used for heat transfer. In Kedida et al.'s [20] study, the cooking pot was place directly on top of the TES unit for cooking and use hot air for thermal charging. Its operating temperature could reach 450 °C. In addition, the cooking unit is different from above that more other types of cooking units that also there are G. Kumaresan et al. studied a Tava cooking unit [21] and a flat plate cooking unit [22]. The operating temperature of thermal oil T55 is around 170 °C.

However, based on the above systems, there are still problems that should be figured out to meet indoor cooking purposes closer: (1) high operating temperature definitely causes much heat loss, so thermal insulation is essential to improve the thermal performance of the system; (2) to meet the cooking demand after sunset and next day morning, a TES unit can be employed to store adequate heat so that to supply for cooking when it needs anytime. By the way, in many solar heating industry processes, the TES technology is relied on to maintain stability and continuity of production. As all know, solar power plant technology has entered the commercial stage, it is usually a large-scale storage unit that uses PCMs as the storage media. The high specific heat capacity materials usage can reduce the storage tank volume, increase system performance and save cost. The application of the SCSs is the same. PCMs have become the popular option to be the filler materials of thermal storage [13,23,24]. G. Kumaresan et al. [21] studied an indirect solar cook system with energy storage using the TES material is used as the PCM ball. The experiment results demonstrated that the overall system efficiency and cooking unit efficiency were 10.2% and 73.5%, the most heat loss incurred in the piping circle and energy storage were found to be 54.3% and 25.3%, respectively. Solving the heat loss problem is the key to improving the whole cooking unit's performance. However, the weaknesses of using PCMs as a storage material are the low heat conductivity coefficient. When the material drops to the melting point, the solidified fluid is adverse to the liquid fluid flow and heat transfer. Meanwhile, to promote the heat transfer of the PCMs, the working device usually is more complicated than which uses the common fluid, thus the processing and manufacturing cost is higher. For the domestic-scale SCS, using a sensible heat storage system of simple structure and easy control is more competitive. There are two common methods of sensible heat storage: (a) two-tank storage, (b) single-tank thermocline storage [25], where the filler materials in the thermocline storage tank can be HTF or rock [26]. The selection of storage materials is quite important because it takes up a large part cost of the entire system, but also its physical properties influence the system effect of heat storage and release. A techno-economic study comparing the packed-bed rock storage and two-tank storage with thermal oil T55 and rapeseed oil as HTF for cogeneration plant indicates the configuration of packed-bed rock with T55 as HTF get the lowest levelized cost of electricity (LCOE) [27]. Karem Elsayed Elfeky et al. [28] studied four kinds of solid materials as filling materials used in the thermocline storage tank, are quartzite, BOF-slag, magnetite, and river rock. Quartzite was found to be the third most economical but has the best TES behavior. Hao Zhou et al. [29] through experiment studied the physical properties of sinter, aluminum oxide ball and rock. Rock is the best choice for thermal storage when the operating temperature is below 550 °C. Kedida et al. [20] studied a pebble bed thermal storage unit and uses air as the heat transfer fluid by simulation, which has the thermal storage capacity of 40.1 MJ. The storage efficiency reaches 66.7% and the overall efficiency of cooking was 30% at the highest DNI day, but for the day with the lowest DNI, these efficiencies are 70.9% and 22.08%, respectively. The research on using the rock to store energy for cooking is rare, especially quartzite. There is no relevant study so far.

The solar collector is the core component of the SCS. Cheng Zheng et al. proposed two double lens concentrators with a thickness of only 8.96 cm and 9.73 cm, which can easily integrate into buildings [30]. A medium-temperature solar collector with a large receive angle, concentration ratio of 4.3 and thickness of 13.2 cm designed by Qiyuan Li et al, the thermal efficiency can reach 46% under the test condition of G = 850 W/m^2 and 200 °C operating temperature [31]. Moucun Yang et al. designed a micro parabolic trough collector (MPTC) which can achieve a concentration ratio of 4.2 in a 150 mm height, the simulation and experiment revealed the collector unit annual optical efficiency is 66.7% and thermal efficiency is 59.3% at 200 °C [32].

In summary, previous studies have clearly revealed the performance of various solar cookers, but little has been reported on the feasibility and economics studies of domestic-using. In addition, Katlego lentswe et al. [33] reviewed solar cookers with heat storage units and indicated that most studies presented on solar cookers are experimental with limited numerical studies. Based on the above, this paper studied a domestic-scale SCS, which consists of the solar collector unit, TES unit and cooktop unit. The novelty and contributions of this study include:

(1) A low-profile solar collector was installed on the rooftop for energy collection. A cooktop unit had been designed to enable indoor cooking, and the operation habit is consistent with using conventional cookers, such as gas electricity. In addition, a rock-bed storage unit had been studied to store thermal energy for cooking, the quartzite and the thermal oil T55 were used as the TES material and HTF, respectively.
(2) The system configurations of which the solar collector areas, thermal storage days (TSD) and heat loss coefficient (HLC) of the storage tank were studied for the annual running performance of SCS, the economy of the SCS was analyzed. At the same time, the single-tank and two-tank storage units, which use the thermal oil T55 as storage material and heat transfer fluid (HTF) were compared with the rock-bed storage unit.

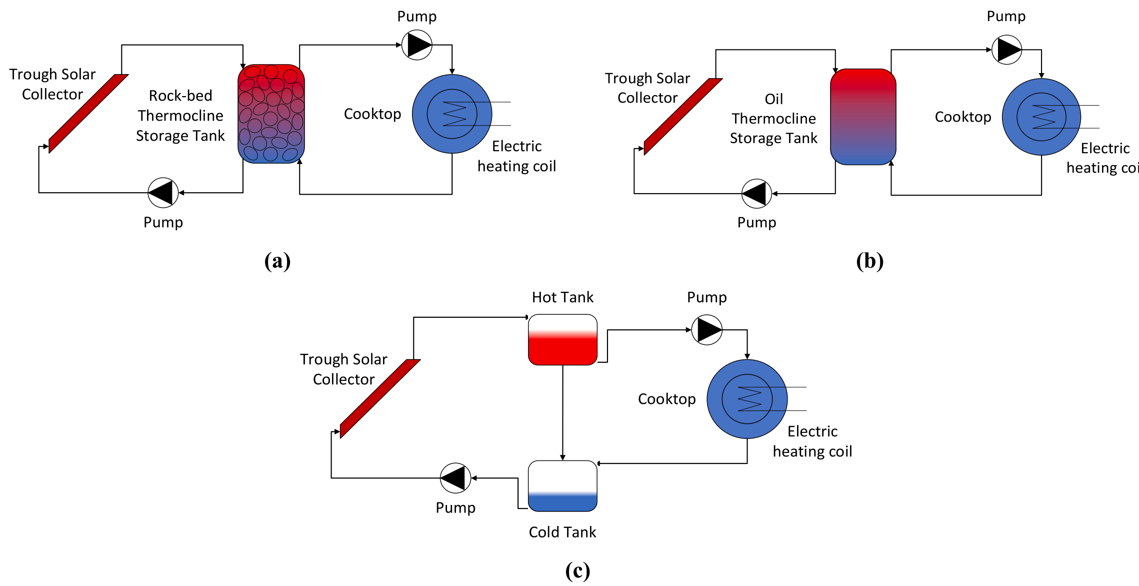

Fig. 2. Simplified schematic of solar cooking systems using different storage methods: (a) rock-bed thermocline storage, (b) single-tank thermocline storage, (c) two-tank storage.

2. Solar cooking system description

The schematic of the SCSs with different types of TES units is shown in Fig. 2. The TES unit is connected with the solar collector to form a thermal charging circuit and connected with the cooktop unit to form a thermal discharging circuit. Each circuit has a pump that drives the HTF to gain solar energy and release heat in the cooktop, and the extra heat will be stored.

The solar collector unit is expected to install on the rooftop to avoid the occupation of land resources. The novel MPTC which has a compact structure and can be installed on the rooftop and integrated with the wall of a building was developed [32] and is now employed to generate a temperature of around 200 °C heat for cooking in this study. To maintain the original cooking habits, a cooktop that is similar to the electric cooktop in the appearance of the structure but works by the HTF flowing and releasing heat inside the cooktop had been designed, the model is shown in Fig. 3. Definitely, the design of cooktop inside can be implanted an electric coil as auxiliary power when the stored heat is exhausted so that it works for cooking by electricity heats the HTF. Three parallel inlets are on one side of the cooktop's main body and one outlet on the opposite side. The top is the cooking surface which is made of a copper plate of 260 mm diameter and welded with conducting fins of 1.5 mm thickness. The main body is a 220 mm diameter cylinder, where the HTF passes and transfers heat to the top cooking surface via the conducting fins. According to the energy balance design for SCS in this paper, the 200 °C HTF flows out from the storage unit to the cooktop, after releasing and flowing out of the cooktop that the temperature drops down to 150 °C, and then it flows back to the storage unit. For the TES units of rock-bed and single-tank, the hot and cold fluids are present in a storage tank but are separated from each other by a thermocline. Usually, the temperature decreases as the height of the tank decreases, so it can be divided into the hot zone, thermocline and

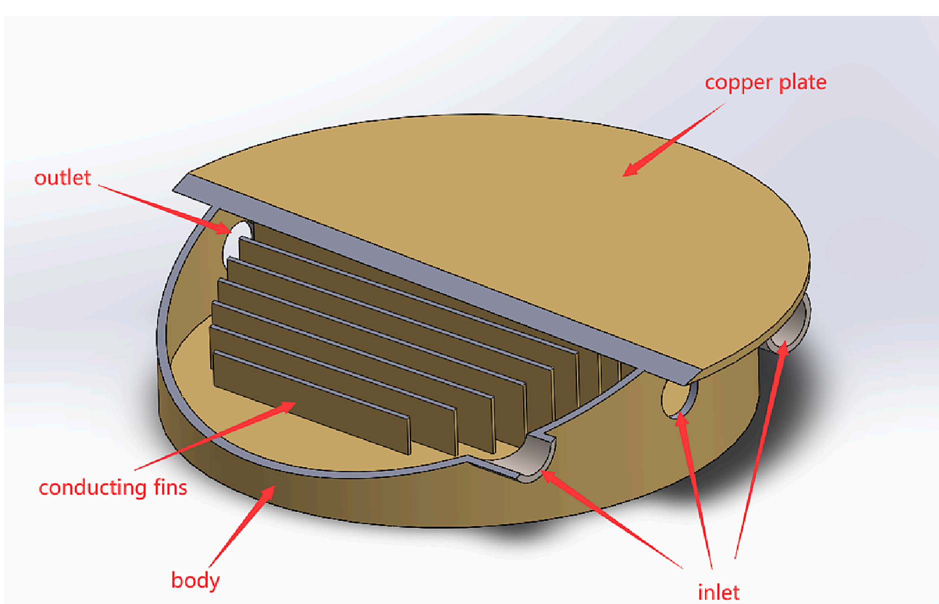

Fig. 3. Part sectional view of the cooktop unit model.

cold zone, respectively. When the storage unit is under the charging process, the cold HTF flows from the storage tank bottom into the solar collector and is heated to setpoint temperature and then stored in the hot zone of the tank. During the discharging process, the hot HTF after releasing heat becomes a cold HTF and flows back to the cold zone at the bottom of the storage tank. But the two-tank storage unit stores the hot HTF and cold HTF separately. In the single-tank thermocline storage unit and the two-tank storage unit, thermal oil T55 is used as the TES material and the HTF. And in the rock-bed thermocline storage unit, the rock material of thermal storage is quartzite and the HTF is T55.

3. Solar cooking system modelling

Based on a family of four, this study assessed the household's energy consumption as the basis for the design of the SCS. Before modelling in the software environment, mathematical models built to calculate and confirm a few key parameters. Then a CFD model in SimScale [34] was built to analyze the heat transfer performance of the cooktop, and SCS models in TRNSYS were used to study the annual performance of SCS. To simplify the system model, the following assumptions were taken to the studied SCS:

(1) The family of four consumes a volume of 30 m^3 of natural gas for monthly cooking activities, and cooking is conducted daily.
(2) When the foods can be judged as cooked, the conventional cooker and SCS have the same effective energy consumption.
(3) The family spends 2.5 h in cooking every day, the distribution of hours is 0.5 h in the morning for cooking breakfast between 6:00 to 7:00, 1 h between 12:00 to 13:00 for cooking lunch and 1 h between 18:00 to 19:00 for cooking dinner, respectively.
(4) Introduce the ideal incident angle modifier (IAM) model to the solar tracking system of MPTC, the solar radiation is always incident perpendicularly on the collector.
(5) The effect of pump's energy consumption and heat loss on the SCS running performance is ignored (heat loss power of pump was estimated to take less than 1% of total input power when it insulated).
(6) The specific heat capacity of the absorber, heat storage container and cooktop are ignored (these impacts were estimated less than 1.6% to the SCS in this study).

3.1. Assessment and comparison of energy consumption

The energy used by conventional cookers is natural gas, LPG and electricity, and the common cookers have gas cookers and electric cooktops. For the comparison purpose with the conventional cookers, the monthly effective energy consumption of cooking was qualified based on the gas cooker's monthly gas consumption and its efficiency. Because assumed the conventional cookers have the same effective energy consumption with CSC, the energy consumption of electric cooktop and total energy input requirement of the CSC are easily known by their system total efficiency. The Chinese national standard GB 16410–2020 [35] stipulates that domestic gas cookers' performance requirement reaches at least 53% efficiency when the smoke suction and exhaust equipment is in operation. The electric cooktop efficiency is around 70%. For the efficiency of SCS, Eq. (1) indicates the system efficiency is equal to the product of the solar collector unit, TES unit and cooktop unit. In this study, the efficiency values of each unit refer to the real data obtained by previous experimental studies. These values were used in the study through a conservative process. The efficiency of solar collector, TES and cooktop units are 50% [32], 70% and 70% [21], respectively. The evaluation and comparison results of energy consumption of the three types of cookers as shown in Table 1.

Table 1
The assessment and comparison of energy consumption of three types of cookers.

Item	Unit	Gas cooker	Electric cooktop	Solar cooking system
System total efficiency	%	53	70	24.5
Monthly gas consumption	m^3	30	–	–
Monthly electricity consumption	kWh	–	230	–
Monthly equivalent input energy/energy consumption	MJ	1093.2	827.7	2364.9
Daily equivalent input energy/energy consumption	MJ	35.9	27.2	77.8
Daily effective energy for cooking	MJ	19.05	19.05	19.05

3.2. CFD simulation setup for cooktop unit

The CFD simulation study is to inspect the heat transfer performance of the cooktop and the reasonability of its design, further which can instruct the optimization and improvement of the internal structure of the cooktop. In SimScale, the imported geometric structure of the cooktop was defined as two domains, e.g., the entity part was defined as the solid domain, which includes the copper plate, body and conducting fins; and the internal cooktop is a cylindrical fluid flow channel, which was defined as the fluid domain. The mesh independence had been verified and the final amount of mesh is determined to be 0.38 million for the simulation. Due to the daily equivalent input energy of the cookers presented in Table 1, and the cooktop's theoretical HTF mass flow rate can be calculated using Eq. (10) to be 0.035 kg/s. Other key parameters can be seen in Table 2.

3.3. Mathematical model of solar cooking system

In this section, the mathematical methods adopted to unscramble the simulation model which will be built in TRNSYS. Based on the law of conservation of energy and followed with the assumption that the heat loss from the pipeline can be ignored, the energy balance equation of the system can be described as:

$$E = \frac{E_{SC}}{\eta_{th}} = \frac{E_S}{\eta_{th}\eta_{S,c}} = \frac{E_C}{\eta_{th}\eta_S} = \frac{E_{C,e}}{\eta_{th}\eta_S\eta_C} \tag{1}$$

It is worth noting that the heat charging, retention and discharging processes of the TES unit all have heat loss. Where $\eta_{S,c}$ is the storage unit charging efficiency, η_S is the thermal storage efficiency of the storage unit, which has considered the heat retention and heat discharging process.

3.3.1. Solar collector

Owing to the solar collector unit is introduced the ideal IAM, the thermal collection normalized efficiency curve of the MPTC is written as Eq. (2) and (3) [32].

$$\eta_{th} = \eta(0,0) - a_1 T^* - a_2 (T^*)^2 \tag{2}$$

Table 2
Input parameters of boundary condition in solar cooktop CFD simulation.

Item	Value	Unit	Justification
Inlet mass flow rate	0.0117	kg/s	Three inlets, a third of total flow rate
Inlet temperature	200	°C	Designed inlet temperature
Outlet pressure	101.3	kPa	[22]
Heat transfer coefficient of the cooking surface	100	W/m^2 K	[22]
Initial boundary temperature	20	°C	–
Ambient temperature	20	°C	–

$$T^{*}=\frac{\frac{T_{in}+T_{out}}{2}-T_0}{I_b} \tag{3}$$

In real experiment and working condition, the energy received power of the solar collector is expressed by Eq. (4).

$$\dot{Q}_{SC}=I_b\bullet A=\frac{\dot{m}_{SC}C_p(t_{out}-t_{in})}{\eta_{th}} \tag{4}$$

3.3.2. Thermal energy storage unit

Once the heat storage demands and the properties of the TES materials are confirmed, the volume of TES tank can be calculated by Eq. (5) [36]. However, the filling material and HTF material of the single-tank thermocline storage unit and two-tank storage unit are both thermal oil T55. Hence, the value of ε should be 1 here.

$$V=\frac{E_{S,d}}{\left[\rho_R C_{p_R}(1-\varepsilon)+\rho_0 C_{p_O}\varepsilon\right](T_H-T_C)} \tag{5}$$

Because of the high operating temperature, a large heat loss is inevitable in the TES unit. This heat loss in the TRNSYS simulation environment is nonnegligible and the simulation component of the TES unit requires the HLC of the 'storage tank' to compute its heat loss energy. The overall HLC can be obtained by Eq. (6).

$$U_{loss}=\frac{1}{R}=\frac{1}{\frac{1}{h_f}+\frac{\delta_T}{k_T}+\frac{\delta_{ins}}{k_{ins}}+\frac{1}{h_o}} \tag{6}$$

It should be noted that the equation of U_{loss} above is not entirely suitable for the two-tank storage unit. The equation expresses the wetted loss coefficient, which is used to calculate the heat loss from the part of the tank which is in contact with the fluid. On the contrary, there is the dry loss coefficient represents the loss coefficient of that part of the tank which is not in contact with fluid. Difference from the wetted loss coefficient, the heat transfer resistance in the equation of dry loss coefficient should add an additional term, $\frac{1}{h_{fo}}$. Hence, it is calculated by using Eq. (7).

$$R_{dry}=\frac{1}{h_f}+\frac{1}{h_{fo}}+\frac{\delta_T}{k_T}+\frac{\delta_{ins}}{k_{ins}}+\frac{1}{h_o} \tag{7}$$

Furthermore, for the thermocline storage unit, the tank is divided into N mixed isothermal segments of equal volume, where each segment interacts thermally with the nodes above and below through fluid conduction and fluid movement [37]. The equation (8) is used to describe this balance between nodes in the following [31,38]:

$$M_iC_p\frac{dT_i}{dt}=\dot{m}_{SC}C_p(T_{i-1}-T_i)-\dot{m}_CC_p(T_{i+1}-T_i)-U_{loss}A_i(T_i-T_a) \tag{8}$$

3.3.3. Cooktop unit

The HTF releases heat in the cooktop and its power can be calculated using Eq. (9).

$$\dot{Q}_C=\dot{m}_CC_p\left(t_{C,in}-t_{C,out}\right) \tag{9}$$

The total energy supplied to cooktop can be calculated using follows Eq. (10).

$$E_C=\frac{E_{C,e}}{\eta_C}=\dot{Q}_C\tau=\dot{m}_CC_p\left(t_{C,in}-t_{C,out}\right)\tau \tag{10}$$

3.4. TRNSYS simulation model of solar cooking system

The simulation models of the SCS with different storage units were built in the TRNSYS environment. The schematic of the simulation model with different storage methods is shown in Figs. 4–6. For the SCS with rock-bed storage unit, the rock-bed was modelled using 'type 10′ model component representing a cylindrical steel storage tank full of

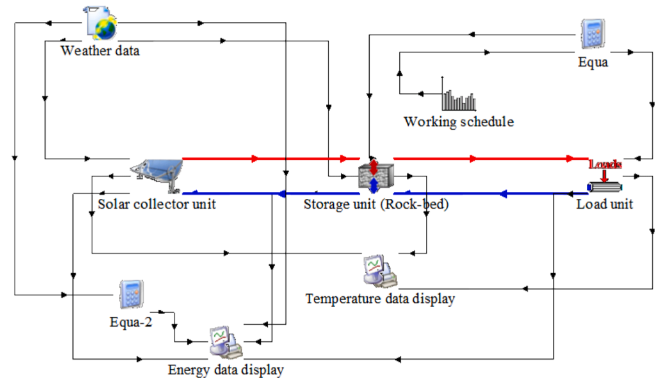

Fig. 4. Simulation model of solar cooking system with rock-bed thermocline storage.

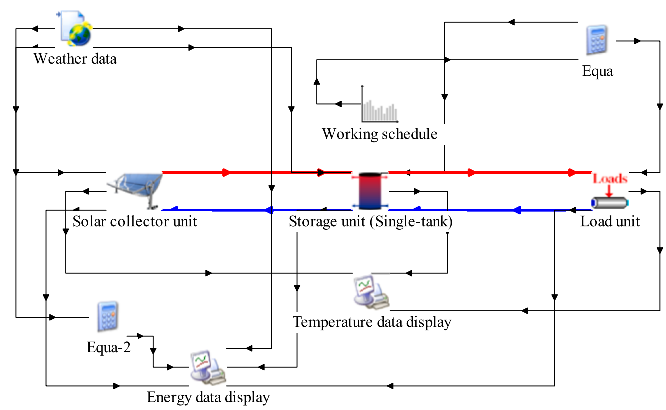

Fig. 5. Simulation model of solar cooking system with single-tank thermocline storage.

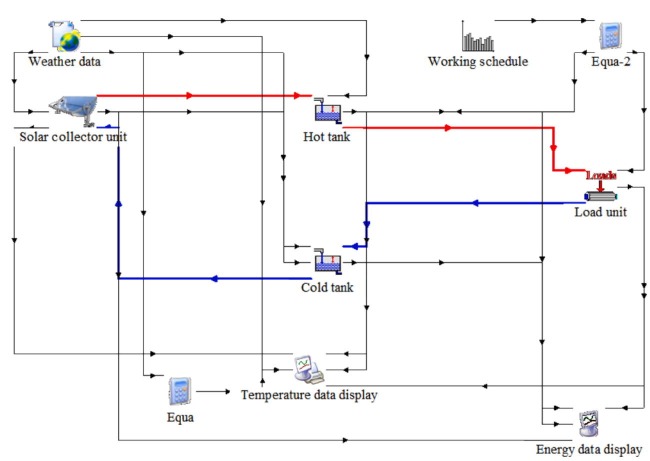

Fig. 6. Simulation model of solar cooking system with two-tank storage.

quartzite and thermal oil T55. The insulation material completely wraps the tank to reduce heat loss. For the configuration of single-tank thermocline storage, the thermocline tank was modelled using 'type 534-NoHX' model component. Their HLC of the storage tank can be calculated by Eq. (6). For the configuration of the two-tank storage unit, the storage tanks were modelled using 'type 39′ model component. The heat transfer resistance of the storage unit can be obtained by Eq. (7). The MPTC was modelled using 'type 1245′ model component. There is not a model component of the cooktop unit in TRNSYS, but according to the working principle of the cooktop is a heating process, 'type 682′

component can be used to model the cooktop because it can simulate the user-specified heating and cooling load input to the flowing fluid and calculate the resultant outlet fluid conditions. There are other model components, such as 'type 15′ component was used for weather data reading and processing, 'type 1243a' model component was modeled to define the working schedule (hourly load condition) of the cooktop, 'Equa' model was used to change the unit of gallon/hour to kg/h, 'Equa-2′ model was used to calculate the solar radiation energy, and the simulation results (include: temperature, fluid mass flow rate and energy rate) were summarized and printed by 'type 65a'.

The SCS installed on the roof of a family in Zhangjiakou city, China was modelled and studied. The EPW format weather data file of Zhangjiakou was obtained from CBE Clima Tool [39], and the data of the observation and statistical year from 1957 to 2021 has been selected.

Before the simulation running, the parameters for each model component were preset. There are three main variables in the study considered to simulate and discuss the annual running performance of the SCS, which are the number of solar collector units (or the total aperture area of the collector), the TSD (or the storage tank volume) and the HLC of the storage unit, and they are shown in Tables 3–6. The input parameters of storage tank volume in Table 4 represent the days on which the TES capacity is enough to support the SCS working continuously, which are 1 day, 3 days and 5 days, respectively. An aspect ratio of 3 was adopted to maintain the stability of thermal stratification in the thermocline tank [40]. The high aspect ratio may also bring a problem in the storage tank higher than the residential building, but based on this research case, the thermocline storage tank can be installed in a 3 m high building even though the largest storage volume is chosen. As for the two-tank storage unit, due to the temperature of the storage medium stored in the tanks being relatively uniform, this tank aspect ratio of 1 minimizes the storage tank surface area and help reduce heat loss. The void fraction of the rock-bed filled quartzite uses 0.27 [41] and the thermal storage temperature range is 150–210 °C. Table 5 presents the working schedule of the cooktop unit under different situations. In general, the SCS can cook for breakfast, lunch and dinner every day, but in months when the solar radiation is too low to meet the demands of all-day cooking, the daily meals cooked by SCS could be reduced depending on the solar energy input to the SCS.

Finally, the criterion for determining the start and end of the simulation running is: if the selected date happens to be the day on which the system can start normally (the storage unit outlet temperature is at 200 °C or above during cooking) and run continuously, this date was determined as the start day of the simulation run. If the simulation goes to such a date on which the storage unit outlet temperature drops to below 200 °C in the year, this day is determined as the finish day of the simulation run.

3.5. Economic analysis model

A detailed levelized cost of cooking energy (LCOC) formula was applied for the economic analysis of the SCS, as given by Eq. (11) [31,32], which takes into account the capital cost (CC) of the entire SCS, system maintenance cost (SMC, includes the average annual cost of HTF maintenance/change and annual solar collectors maintenance cost) and the annual total input energy for cooktop.

Table 3
Input parameters of solar collector for simulation of solar cooking system.

Parameter	Value	Units
Aperture area	0.86	m^2/unit
Number of collector units	4, 6, 8, 10, 12, 14	units
Intercept efficiency (a_0)	0.64	–
1st order loss coefficient (a_1)	1.00926	W/m^2 K
Outlet temperature setpoint	210	°C

Table 4
Input parameters of thermal energy storage tank for simulation of solar cooking system.

Parameter		Value	Units
Rock-bed thermocline storage	Storage volume	0.28, 0.85, 1.42	m^3
	Heat loss coefficient	0.22, 0.1	W/m^2 K
	Effective thermal conductivity	3.5	W/m K
	Number of nodes	5	–
	Initial temperature of segments	210	°C
Single-tank thermocline storage	Number of nodes	6	–
	Storage tank volume	0.41, 1.24, 2.07	m^3
	Heat loss coefficient	0.22, 0.1	W/m^2 K
	Initial tank temperature	210	°C
Two-tank storage	A tank volume	0.41, 1.24, 2.07	m^3
	Wetted heat loss coefficient	0.22, 0.1	W/m^2 K
	Dry heat loss coefficient	0.08, 0.056	W/m^2 K
	Initial temperature (hot tank/cold tank)	210/150	°C

Table 5
Input parameters of cooktop unit schedule for simulation of solar cooking system.

Meals	Parameter	Value	Units
All-day cooking (100% cooking)[a]	Daily total circular oil volume	0.413	m^3
	06:00 to 07:00	0.2	Fraction
	12:00 to 13:00	0.4	Fraction
	18:00 to 19:00	0.4	Fraction
Breakfast & lunch (60% of all-day cooking)[b]	Total circular oil volume	0.248	m^3
	06:00 to 07:00	0.3333	Fraction
	12:00 to 13:00	0.6666	Fraction
Lunch (40% of all-day cooking)[c]	Total circular oil volume	0.165	m^3
	12:00 to 13:00	1	Fraction
Breakfast (20% of all-day cooking)[d]	Total circular oil volume	0.083	m^3
	06:00 to 07:00	1	Fraction

[a] Cooking for breakfast, lunch and dinner.
[b] Cooking for breakfast and lunch.
[c] Cooking for lunch.
[d] Cooking for breakfast.

Table 6
Input parameters of the properties of storage filler material.

Parameter		Value	Units
Thermal oil T55 [42]	Specific heat capacity of fluid	2.455	kJ/kg K
	Density of fluid	766	kg/m^3
	Thermal conductivity of fluid	0.11	W/m K
	Viscosity of fluid	0.001021	kg/m s
	Thermal expansion coefficient of fluid	0.00096	1/°C
Quartzite [41,43]	Specific heat capacity of rock	1.185	kJ/kg K
	Apparent density of rock bed	2082.92	kg/m^3
	Effective thermal conductivity	3.5	W/m K

$$LCOC = \frac{CC \times CRF + SMC}{E_{C,a}} \tag{11}$$

where the capital recovery factor (CRF) is defined in Eq. (12).

$$CRF = \frac{i \bullet (1+i)^n}{(1+i)^n - 1} \tag{12}$$

where the i is the annual interest rate and n is the design life time.

It is similar to LCOC, a model of LCCM is introduce to SCS as a part of economic analysis and that can be used to evaluate the cost for cooking a 'standard' meal with a certain cooker, and the equation can be described as [44,45]:

$$LCCM = \frac{CC \times CRF + SMC}{M_l} \tag{13}$$

And the SF is defined as the contribution ratio of solar energy to the total energy requirement, and it can be calculated by Eq. (14).

$$SF = \frac{annual\ electricity\ savings\ by\ solar}{annual\ electricity\ consumption} \tag{14}$$

4. Technological analysis of system

4.1. Results and discussion for CFD simulation of cooktop unit

The heat transfer simulated study of the cooktop was under the non-cooking load, meaning the cooking surface of the cooktop merely transfers heat to the environment medium. The simulation results show when the cooktop reaches steady a state that, the average temperature of the cooking surface and outlet temperature is at 160.8 °C and 184.9 °C, respectively. If there is no insulation on the cooktop body and bottom, the temperature of the cooking surface and average outlet temperature is reduced to 157.1 °C and 182.9 °C respectively. Fig. 7 and Fig. 8 display the cross-section temperature contours of the cooktop. It can be found that the green area in conducting fins of the cooktop without insulation is larger than the one with insulation and the color legend shows the temperature of the cooktop without insulation is lower, which means the internal heat transfer of the cooktop without insulation is fast. In terms of the body and bottom area of the cooktop, comparing the two figures also illustrates that the cooktop with thermal insulation measures the temperature much higher than without thermal insulation. Because the heat will be transferred to the copper plate, cooktop bottom and body, although the diameter of the cooking surface had been designed to be larger than the cooktop body, the surface area is less than the non-cooking surface, which is the sum of areas of the body and the bottom of cooktop, which will lead to a part of heat lost from the non-cooking surface to environment. To increase energy efficiency, it is desirable to transfer as much heat as possible to the cooking surface, the thermal insulation for the cooktop is a significant step. Fig. 7 and Fig. 8 also show that the highest temperature is located near the cooktop's center, which illustrates that the internal structure design is in favor of the HTF flowing and the heat transferring to the cooking surface. In addition, in real cooking activities using the SCS and if the outlet temperature is around 150 °C, according to Eq. (9) is known that the real output power of the cooktop is controllable with the change of cooking load by changing the inlet mass flow rate.

4.2. Results and discussion for solar cooking systems simulations

Under the effect of the three controlled variables, the annual running simulation results of the SCS can be seen from Figs. 9–11, the figures illustrate the available operation days of which the SCS with three types of storage units serves all-day cooking. And also, it can be seen in the figures that there are some points fall onto the curves, which means the SCS under the corresponding variables had been interrupted intermittently during the year due to weather condition.

Comparing shows that the effect of solar collector area on running days is significant for the SCS with rock-bed storage and single-tank storage, the longest running days can be over 330 days. With the increasing solar collector area that the growth rate of the running days of SCS with two-tank storage tends to be gradual, the longest running day is under 300 days. Meanwhile, the solar collector outlet temperature was set to 210 °C generally and the SCS can be operated in the temperature range of 150 °C to 200 °C. But in some exceptional cases, the solar collector outlet temperature is enhanced to maintain the SCS operation temperature in this range. These exceptional cases commonly appear in the SCS with two-tank storage.

Moreover, the insulation is essential to the long-term TES units, especially when the TSD is 3-day and 5-day. When the HLC of the storage tank is 0.1 W/m^2 K there isn't much difference in running days between the different storage of TSD. If the HLC value is 0.22 W/m^2, as shown in the figures, the running days are reduced as the increase of TSD. It can be explained by the higher heat loss during winter, when both ambient temperature and solar radiation are low, and the system's

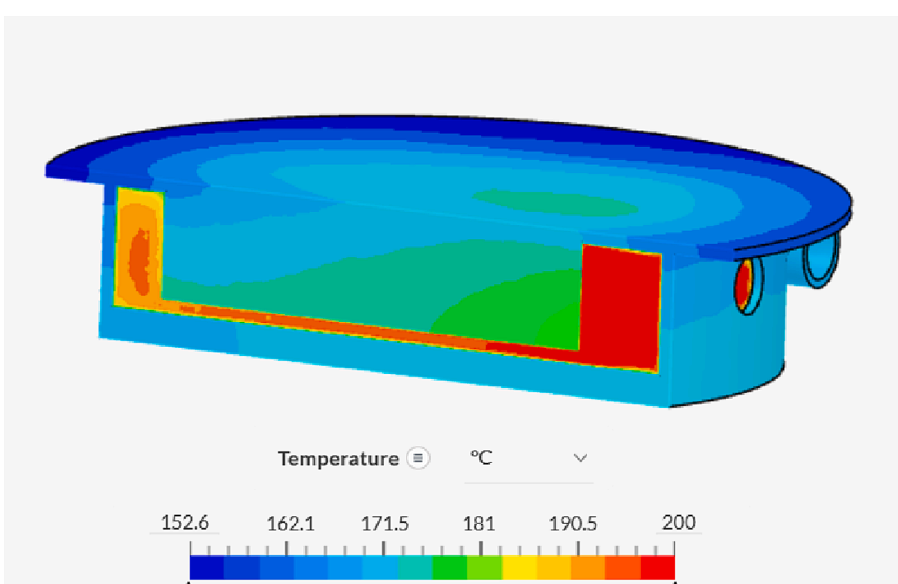

Fig. 7. Temperature distribution of the cooktop (with thermal insulation on non-cooking surface).

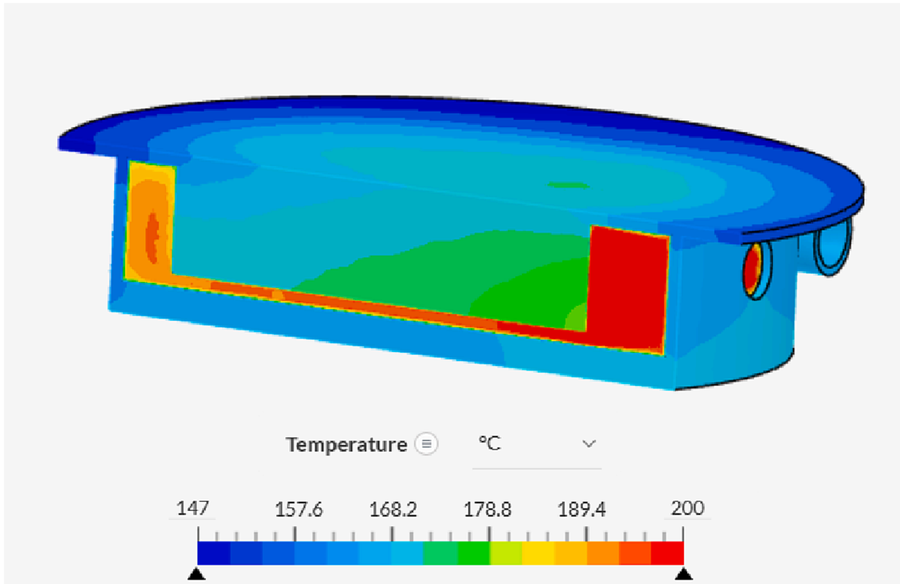

Fig. 8. Temperature distribution of the cooktop (without thermal insulation on non-cooking surface).

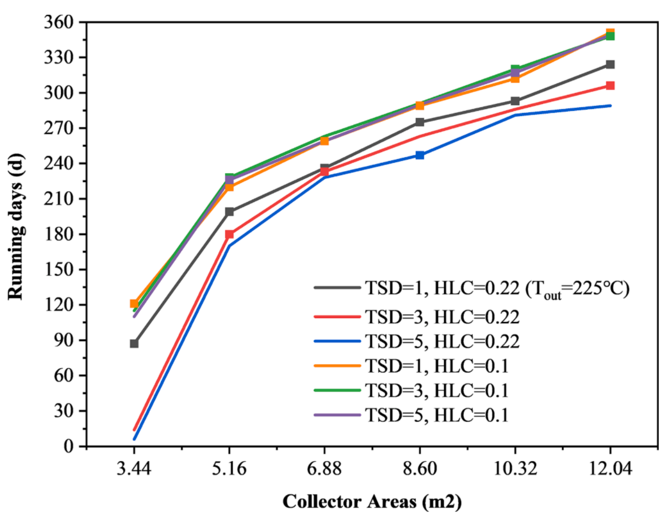

Fig. 9. Running days variation with collector areas for solar cooking system with rock-bed storage.

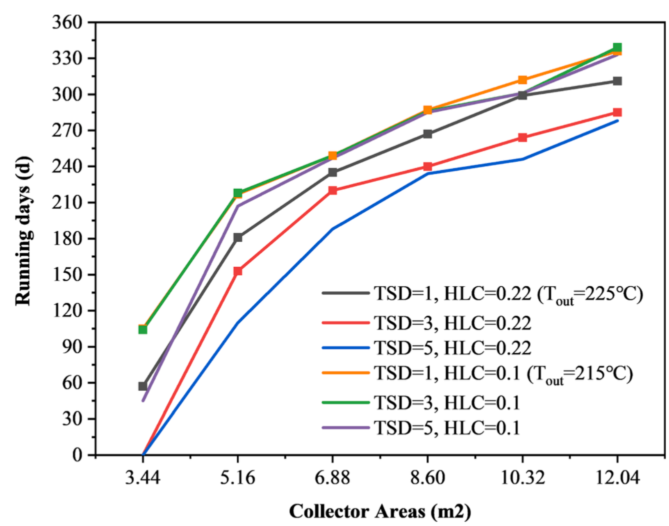

Fig. 10. Running days variation with collector areas for solar cooking system with single-tank storage.

storage volume is larger due to the longer TSD which will lead to higher heat loss from the storage tank, thus the TSD of 5 will early than TSD of 1 and 3 enter the period of a solar energy shortage, resulting in the less running days of long TSD. However, to achieve the HLC of 0.1 W/m^2 K means the thickness of 450 mm insulation should be used for the TES tank, which is unreasonable if installed indoors in domestic houses. Suppose the SCS with short TSD and low HLC is selected to serve for cooking. In that case, the implanted electricity heating coil will ensure the cooking activities when the SCS suffers continuous overcast days and rainy days.

Fig. 12 shows the annual operation of the SCS with rock-bed storage, the employed solar collector areas, TSD and HLC are 5.16 m^2, 1 day and 0.22 W/m^2 K, respectively. The SCS under this configuration can cover the all-day cooking of the entire spring and summer, but not in autumn and winter. Once the SCS runs into the periods of insufficient solar radiation and low ambient temperature that the SCS service capacity is gradually reduced until it can only do breakfast. In the annual running hours, the SCS has been interrupted several times due to the weather condition, but with the increase of TSD this situation will be eased, it can be approved by comparing Figs. 13–15 which takes the running time of 5136 to 5352 h as an example (the area marked by two red dash line in the Fig. 12). Because in this period, the solar cooking system under 100% cooking state and suffers the longest insufficient solar radiation of a whole year. The figures respectively present the running situation of three types of storage methods of CSC during a running interruption. Their solar collector areas and HLC are both 5.16 m^2 and 0.22 W/m^2 K, respectively. Obviously, the storage tank outlet temperature fluctuated wildly for the thermocline storage methods and when the TSD is 1, but the TSD of 3 and 5 are relatively stable. This can be explained as the smaller storage volume outlet temperature has a wide range of variation due to the alternated charging and discharging process, leading to the thermocline moving fast in the storage tank, but the larger storage volume has enough heat supply for cooking, the visualized temperature change of the storage tank outlet is mainly because of the heat loss. When the temperature of the systems drops below 200 °C that the SCS will enter a state which is not meet the operating conditions, the SCS with rock-bed storage and TSD of 1 earlier enters this state around the running time of 5256 h than the TSD of 3 around the running time of

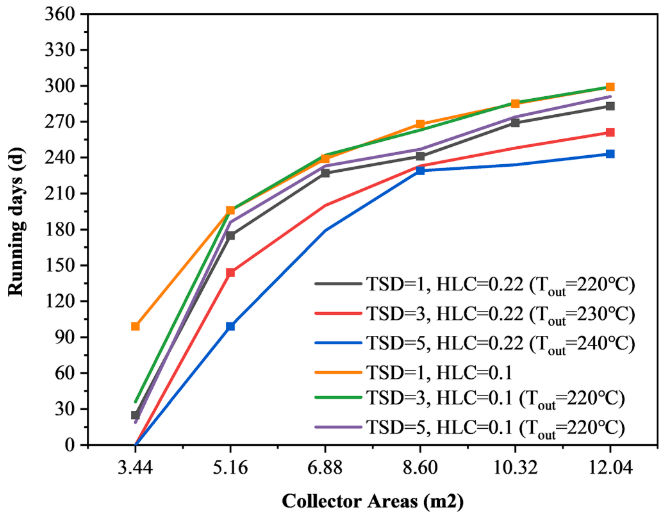

Fig. 11. Running days variation with collector areas for solar cooking system with two-tank storage.

5280 h, and the duration of the TSD of 1 is longer as well, while with the TSD of 5 still in working and the operation temperature around 200 °C. At the same condition, the SCS with single-tank thermocline storage operates at lower temperature than that with the rock-bed. But for the two-tank storage method, it can be found that the temperature of the TSD of 1 plunge to near the ambient temperature, which indicates the hot fluids in the hot tank has been used up. Besides the SCS with TSD of 1, the system working temperature could be close to 200 °C. By comparison, the rock-bed thermocline storage performs better than others.

5. Economic analysis of system

5.1. Initial cost analysis

The initial investment cost of the SCS mainly consists of the cost of the solar collector unit, the TES unit and the cooktop unit. By referring to previous studies and making estimates, the unit price of necessary cost items for each unit of the SCS is summarized in Table 7. And to facilitate the systematic economic analysis in the study, the monetary unit was unified and used the USD consistently. The cost of the cooktop unit is fixed in the initial investment cost of the SCS. The main factors affecting the initial investment cost are the total collector area, the TES unit's storage tank volume, the TES materials' mass, and the insulation materials' thickness and area.

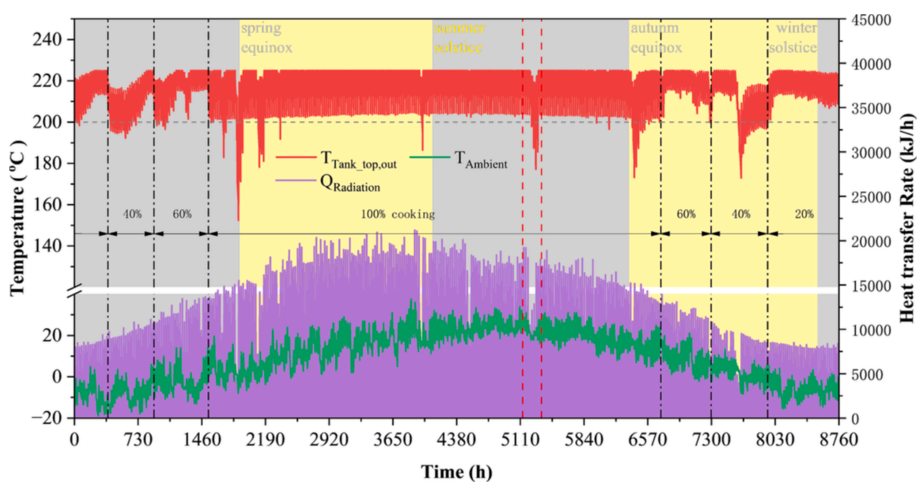

Fig. 12. Simulation of one year operation of the SCS with rock-bed storage.

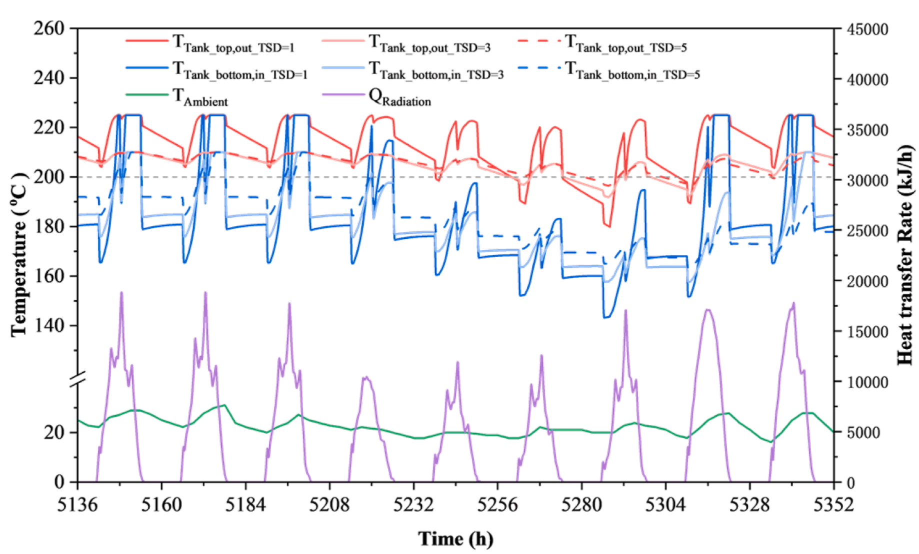

Fig. 13. Dynamic performance of the SCS with rock-bed thermocline storage during one interruption.

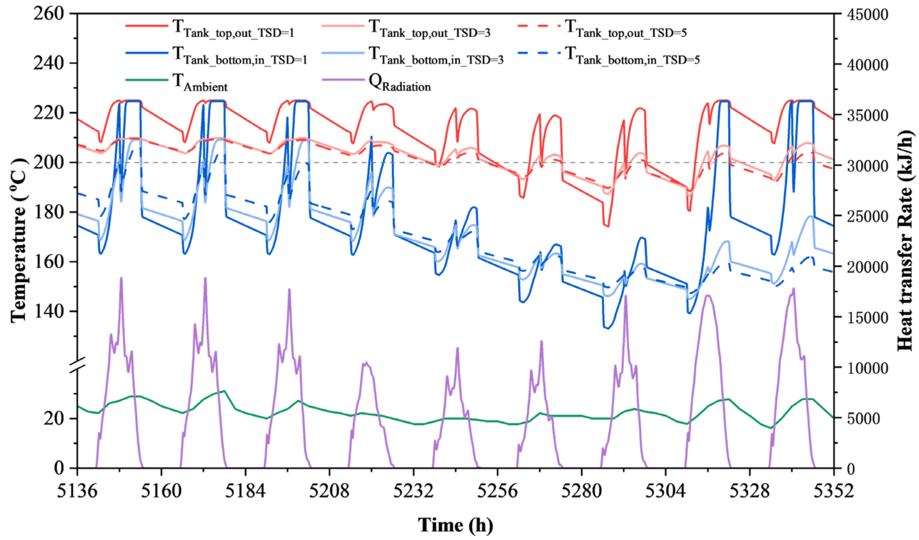

Fig. 14. Dynamic performance of the SCS with single-tank thermocline storage during one interruption.

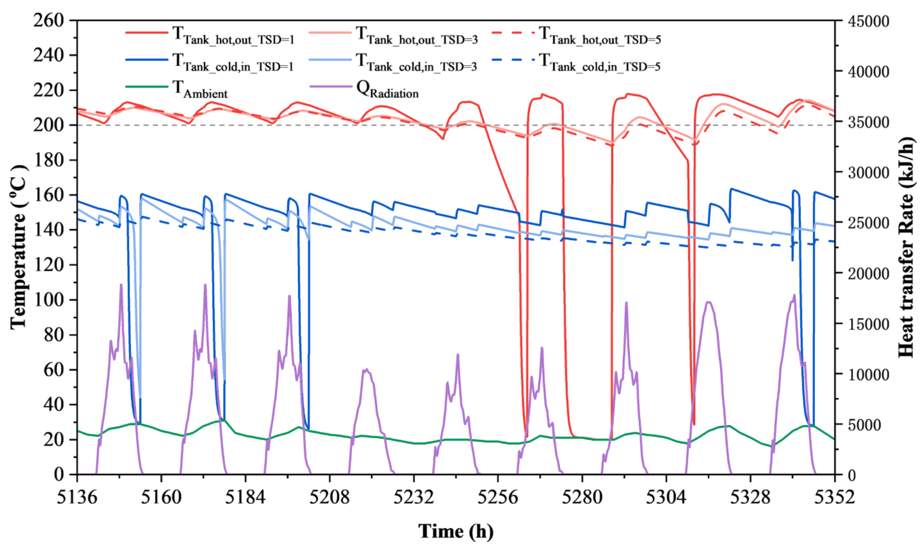

Fig. 15. Dynamic performance of the SCS with two-tank storage during one interruption.

Definitely, the initial investment cost is linearly related to the total solar collector area, the storage tank volume, the insulation area, the mass of TES materials. The total cost of the SCS increase with more collector areas and storage tank volumes used, and the quality of the thermal insulation is improved. The relationship between the total cost and the impacted variables can be seen in Fig. 16. Compared the SCS with three types of storage units, the economic order of their impact on the initial investment cost of SCS is the rock-bed thermocline storage, the single-tank thermocline storage and the two-tank storage. Because the rock-bed thermocline storage unit has a smaller storage tank volume, which saves a little of the cost on the tank manufacture and the insulation area, the TES materials use cheaper quartzite than the thermal oil T55. While the two-tank storage unit has one more storage tank than the rock-bed and single-tank thermocline storage unit, and the cost is significantly higher because of the additional expenditure on the storage tank and insulation.

Nevertheless, the linear cost is unable to reflect the relationship between the system cost and system annual performance. The solar collector area impacts the SCS annual performance markedly, if the variables other than the total solar collector area are determined, there is a functional relationship between the running days and the total solar collector area. Thus, the cost-area relationship can be updated to a nonlinear cost-running relationship, as shown in Fig. 17, which was established with running days as the abscissa and initial investment cost as the ordinate and which presents the relationship between the running days and total cost of SCS with three different TES units visualized. It indicates that the total cost of SCS is increased with the more requirement of running days, two curves of which the TSD are consistent approximately are coincidence. From a total cost standpoint alone, adding solar collector units and improving HLC are the most economical measures to promote the SCS annual running performance.

Therefore, this study concludes that the rock-bed thermocline storage unit of the TSD of 1-day and the HLC of 0.22 W/m^2 K (200 mm thermal insulation) for SCS is the optimum option. And finally, the investment cost and running days are merely impacted by the total solar collector area.

5.2. Comprehensive economic analysis

5.2.1. Capital cost composition

Fig. 18 illustrates the CC composition of the SCS with rock-bed thermocline storage. It could be found that the cost of the solar

Table 7
The unit price list of the initial cost items for solar cooking system.

Item		Value	Unit	Justifications
Solar collector unit	Trough collector module	616	$/unit	[32]
	Extra equipment	109.4	$/set	[32]
Thermal energy storage unit	Storage tank [a]	625	$/m^3	[36]
	Quartzite [a]	0.5	$/kg	[43]
	Thermal oil T55 [a]	2.5	$/kg	[36]
	Tank insulation [b]	40.8	$/m^2	1 layer, 200 mm [46]
	Tank insulation [b]	47.46	$/m^2	3 layers, 3*150 mm = 450 mm [47]
Cooktop unit	Cooktop with insulation	30	$	A reasonable estimate
	Pump	46	$	A reasonable estimate
	Controller	30	$	A reasonable estimate

[a] € to $ exchange rate 1 (July 2022).
[b] £ to $ exchange rate 1.2 (July 2022).

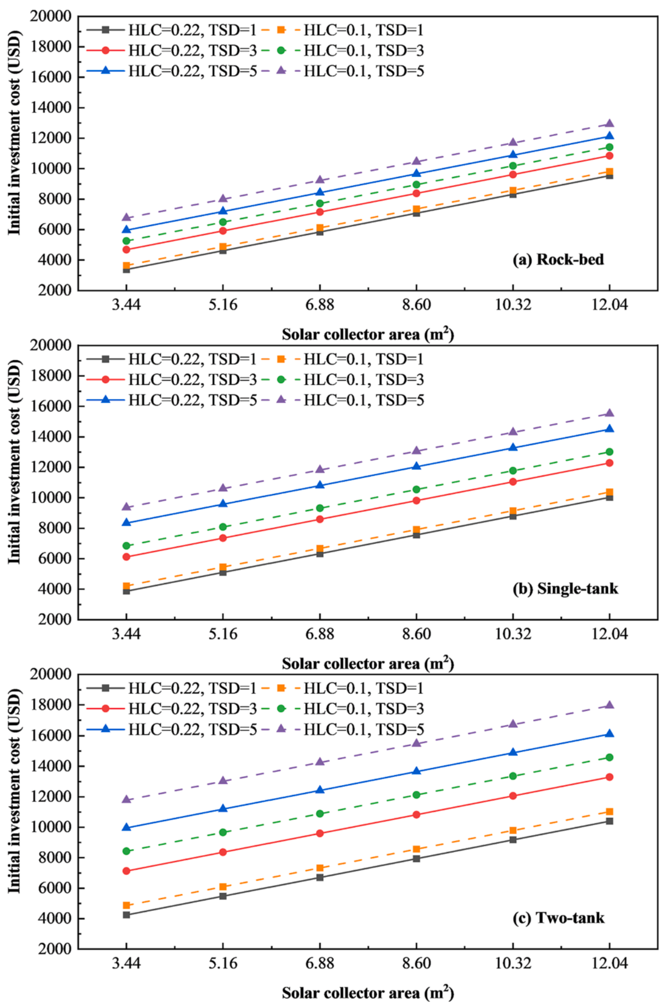

Fig. 16. The linear total cost of the solar cooking system with three types TES units.

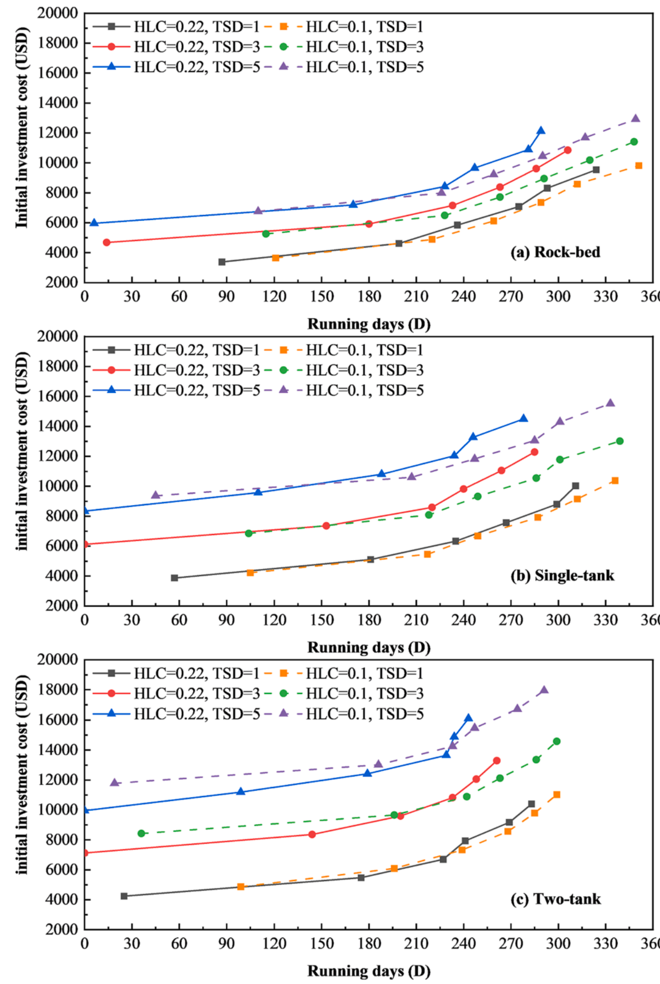

Fig. 17. The nonlinear total cost of the solar cooking system with three types TES units.

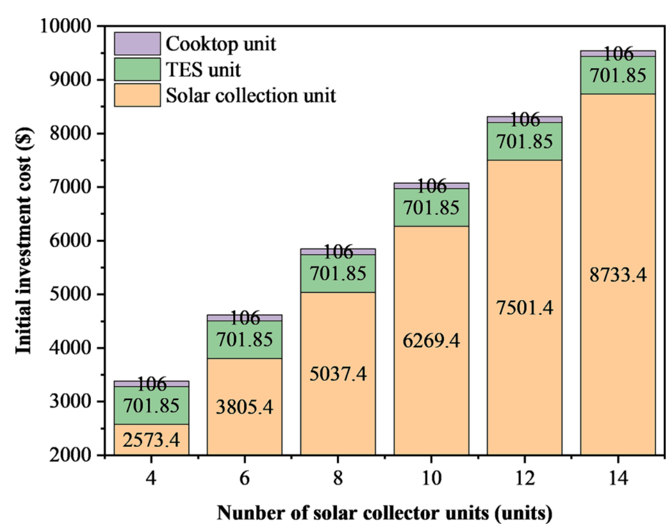

Fig. 18. The capital cost composition of the solar cooking system with rock-bed thermocline storage.

collector unit takes up most of the initial investment cost, the second is the TES unit and the rock-bed thermocline storage unit and cooktop unit occupy the least part of the initial investment cost.

5.2.2. Levelized cost and solar fraction

The calculation and analysis results of the levelized cost and SF are seen in Fig. 19. The LCOC gets to the lowest level when the number of the solar collector units is 6, and then will at the rising trend with the

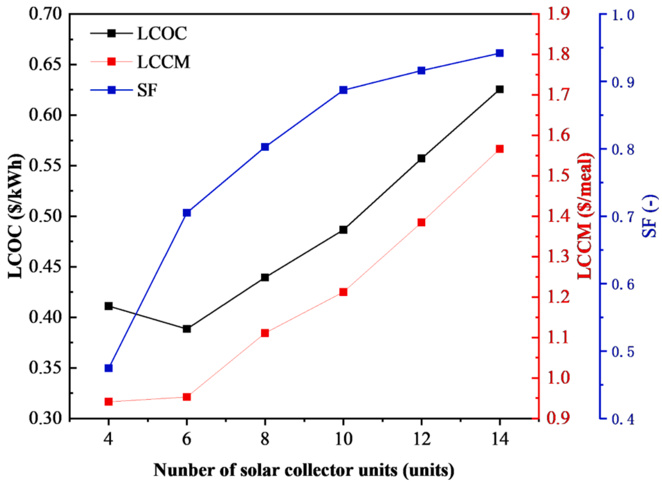

Fig. 19. The levelized cost and solar fraction analysis of the solar cooking system with rock-bed thermocline storage.

number of the solar collector units go up, the LCCM at the rising trend from the start. This needed to be pointed out the difference, because the energy consumption ratio of three meals in a day is 1:2:2 in the calculation of LCOC, whilst the breakfast was counted as a meal rather than a half meal in the calculation of LCCM. The SF is at a rising trend from the start and then the growth rate gradually slows down and it is not difficult to understand the increased SF because of the increased solar collector area so that more radiation is harvested and used. The reason for the decline of LCOC when the collector units are from 4 plus to 6 is that the annual running days of the SCS with 4 solar collector units are reduced considerably so that over the normal level, and further influence the annual saving energy, based on the Eq. (11) knows the LCOC of the solar collector unit of 4 is higher.

In summary, the SCS with rock-bed storage of 6 solar collector units (solar collector areas of 5.16 m^2) is cost-optimal. Assuming the system lifetime is 20 years and the analysis details can be found in Table 8. This SCS has the lowest LCOC of 0.3884 $/kWh, the available working days are 345 annually, of which the 100% cooking days are 199, SF of the system can reach 71%. It is compared to the energy price of natural gas and electricity are 0.05 $/kWh around and 0.0877$/kWh respectively, in Zhangjiakou [48], the LCOC of SCS is 0.3884 $/kWh which is relatively higher. There is only 0.012 $/Meal difference between the number of solar collector units of 4 and 6 in the LCCM. However, the 6 units solar collector has an LCCM of 0.953 $/Meal is still at a very high-cost level compared to the gas cooker and electric cooktops' LCCM of 0.1722 and 0.2279 $/Meal in Zhangjiakou (calculation cost), even also higher than other referable costs of around 0.35 $/Meal [45].

Table 8
The economic analysis of the solar cooking system with rock-bed thermocline storage.

Item	Unit	Value	Justification
Number of collector Units	Units	6	Lowest LCOC
Collector Area	m^2	5.16	Lowest LCOC
100% cooking	Days	199	Simulation result
60% cooking	Days	50	Simulation result
40% cooking	Days	46	Simulation result
20% cooking	Days	50	Simulation result
Annual electricity saving	kWh	1945.68	Calculation result
Annual cost savings	$	170.62	[48]
Design life time	Year	20	Assumption
Annual interest rate	–	0.0445	[49]
HTF maintenance/change	$	441.61	Three times in the life time
Collector maintenance	%	10	[32]
Annual total input energy for cooktop	kWh	1945.68	Calculation result
Annual cooking meals	Meal	793	Simulation result

5.2.3. Environmental benefit analysis

In China, coal-fired power accounts for more than 50% of electricity generation in 2020 [50], while around 1 kg of CO_2 is released for every kilowatt-hour of electricity produced by burning coal [51]. It is assumed that 0.9 kg of CO_2 is released for every 1kWh of electricity produced and 201.96 kg of CO_2 is produced per megawatt-hour of natural gas [52]. Thus, the results of CO_2 savings were shown in Fig. 20, it illustrated the contribution of environmental benefit by the SCS with rock-bed thermocline storage. The carbon emissions from using electricity for cooking are far higher than those from using natural gas. For instance, if a family has an SCS with 6 units of solar collector for cooking, the family could save 1.75 tons of CO_2 per year compared to using electricity and save 0.52 tons per year compared to using natural gas. However, there is still a little difference in the carbon emissions of electricity consumption in various countries, as for the countries in which renewable energy generation takes up a large share of the total power generation, it definitely will be less.

Additionally, the rock-bed thermocline storage unit used in SCS can be more environmentally friendly than the single-tank thermocline storage unit and two-tank storage unit because the thermal oil T55 is both the TES material and the HTF in the single-tank thermocline storage unit and the two-tank storage unit. While the T55 is only used as the HTF in the entire SCS with rock-bed thermocline storage, the TES material uses quartzite which is a harmless natural rock resource with stable physical and chemical properties.

6. Conclusion

This paper studied a domestic-scale SCS which can meet indoor and all-day cooking demands by equipping a TES unit. A cooktop unit similar in profile to the electric cooktop was designed, and an electric heating coil could be implanted to achieve the operation mode the same as the electric cooktop during the SCS stopped working. The CFD simulation was conducted to analyze the heat transfer performance. The simulation model of SCS was built in TRNSYS environment to validate the technical feasibility of the entire system, compared and studied the annual performance of the SCS which configurated three types of storage units respectively. And finally, the economy of SCS was discussed to compare with the conventional cookers.

The study results revealed that the designed structure of the cooktop

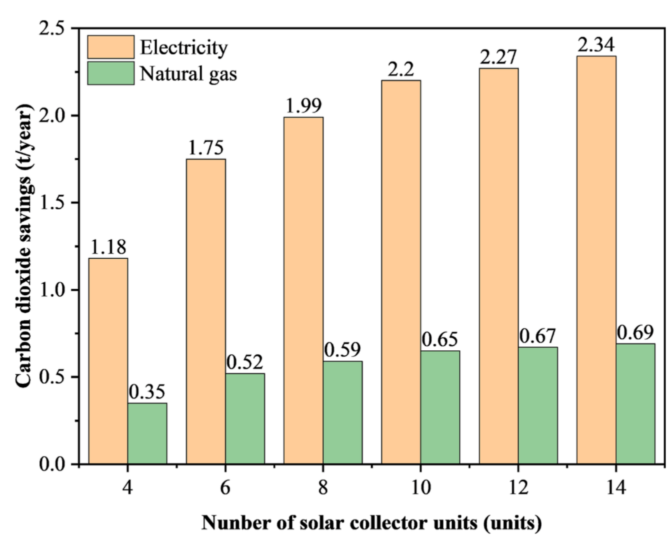

Fig. 20. The environment benefit analysis of the solar cooking system with rock-bed thermocline storage.

has a good heat transfer performance so that it could be used for cooking activities. Furthermore, the study revealed that compared to the single-tank thermocline storage unit and two-tank storage unit, using the rock-bed thermocline storage unit for the SCS will have the longest continuous running days throughout the year, and the SCS with rock-bed thermocline storage unit is also most economic. When the SCS with rock-bed thermocline storage is configurated with the TSD of 1 day, the HLC of 0.22 W/m^2 K and 6 units solar collector, the system could get the lowest LCOC of 0.3884 $/kWh and corresponding LCCM of 0.953 $/Meal. But the CC of per unit of energy is also high relative to conventional sources, such as natural gas and electricity. The system has the SF of 71% and could annually save 1.75 tons and 0.52 tons of carbon emissions, respectively, relative to using electricity and natural gas for cooking. By contrast, the advantage of using the rock-bed storage unit for SCS is apparent. Firstly, it is a benefit for boosting the performance of SCS. Moreover, the heat storage tank has a smaller volume than other TES units, occupies a smaller area, requires less insulation materials, and is the most cost-effective. Finally, owing to the use of natural quartzite to store thermal energy, it is relatively environment-friendly compared to using the thermal oil T55.

In the end, the SCS is still facing the problem of high initial investment cost, the low-cost solar collector and storage unit technology are still the keys to reduce the total cost. At the same time, in the future study, the experiment platform can be set up to further demonstrate the system operation performance. In the economic aspect, the effect of the carbon sink cost on the SCS can be considered and studied.

Declaration of Competing Interest

The authors declare that they have no known competing financial interests or personal relationships that could have appeared to influence the work reported in this paper.

Acknowledgements

This study was supported by the National Key Research and Development Program of China (2018YFB1502900), the Joint Master Program Between University of Hull and Nanjing Tech University.

References

[1] IEA (2022) Data & Statistics. Available online: https://www.iea.org/data-and-statistics/data-browser?country=WORLD&fuel=Energy%20consumption&indicator=TFCShareBySector (Accessed: 4 July 2022).
[2] Saxena, A., Goel, V., Karakilcik, M., 2017. Solar Food Processing and Cooking Methodologies. Springer, Singapore, pp. 251–294.
[3] Li, G., Zheng, X., 2016. Thermal energy storage system integration forms for a sustainable future. Renewable and Sustainable Energy Reviews 62, 736–757.
[4] Lahkar, P.J., Samdarshi, S.K., 2010. A review of the thermal performance parameters of box type solar cookers and identification of their correlations. Renewable and Sustainable Energy Reviews 14 (6), 1615–1621.
[5] Muthusivagami, R.M., Velraj, R., Sethumadhavan, R., 2010. Solar cookers with and without thermal storage—A review. Renewable and Sustainable Energy Reviews 14 (2), 691–701.
[6] Aramesh, M., Ghalebani, M., Kasaeian, A., Zamani, H., Lorenzini, G., Mahian, O., Wongwises, S., 2019. A review of recent advances in solar cooking technology. Renewable Energy 140, 419–435.
[7] Cuce, P.M., 2018. Box type solar cookers with sensible thermal energy storage medium: A comparative experimental investigation and thermodynamic analysis. Solar Energy 166, 432–440.
[8] Tawfik, M.A., et al., 2022. Performance evaluation of solar cooker with tracking type bottom reflector retrofitted with a novel design of thermal storage incorporated absorber plate. Journal of Energy Storage 51, 104432.
[9] Apaolaza-Pagoaga, X., Sagade, A.A., Rodrigues Ruivo, C., Carrillo-Andrés, A., 2021. Performance of solar funnel cookers using intermediate temperature test load under low sun elevation. Solar Energy 225, 978–1000.
[10] Ruivo, C.R., et al., 2022. Influence of the aperture area on the performance of a solar funnel cooker operating at high sun elevations using glycerine as load. Sustainable Energy Technologies and Assessments 53, 102600.
[11] Sagade, A.A., Apaolaza-Pagoaga, X., Rodrigues Ruivo, C., Carrillo-Andrés, A., 2022. Concentrating solar cookers in urban areas: Establishing usefulness through realistic intermediate temperature rating and grading. Solar Energy 241, 157–166.
[12] Zhao, Y., Zheng, H., Sun, B., Li, C., Wu, Y., 2018. Development and performance studies of a novel portable solar cooker using a curved Fresnel lens concentrator. Solar Energy 174, 263–272.
[13] Bhave, A.G., Kale, C.K., 2020. Development of a thermal storage type solar cooker for high temperature cooking using solar salt. Solar Energy Materials and Solar Cells 208, 110394.
[14] Mawire, A., Lentswe, K., Owusu, P., Shobo, A., Darkwa, J.o., Calautit, J., Worall, M., 2020. Performance comparison of two solar cooking storage pots combined with wonderbag slow cookers for off-sunshine cooking. Solar Energy 208, 1166–1180.
[15] Mawire, A., Lentswe, K., Owusu, P., 2022. Performance of two solar cooking storage pots using parabolic dish solar concentrators during solar and storage cooking periods with different heating loads. Results in Engineering 13, 100336.
[16] Kanyowa, T., Victor Nyakujara, G., Ndala, E., Das, S., 2021. Performance analysis of Scheffler dish type solar thermal cooking system cooking 6000 meals per day. Solar Energy 218, 563–570.
[17] Singh, O.K., 2021. Development of a solar cooking system suitable for indoor cooking and its exergy and enviroeconomic analyses. Solar Energy 217, 223–234.
[18] Hosseinzadeh, M., Sadeghirad, R., Zamani, H., Kianifar, A., Mirzababaee, S.M., 2021. The performance improvement of an indirect solar cooker using multi-walled carbon nanotube-oil nanofluid: An experimental study with thermodynamic analysis. Renewable Energy 165, 14–24.
[19] Hosseinzadeh, M., et al., 2021. Experimental study of a nanofluid-based indirect solar cooker: Energy and exergy analyses. Solar Energy Materials and Solar Cells 221, 110879.
[20] Kedida, D.K., Amibe, D.A., Birhane, Y.T., 2019. Performance of a Pebble Bed Thermal Storage Integrated with Concentrating Parabolic Solar Collector for Cooking. Journal of Renewable Energy 2019, 1–12.
[21] Kumaresan, G., Vigneswaran, V.S., Esakkimuthu, S., Velraj, R., 2016. Performance assessment of a solar domestic cooking unit integrated with thermal energy storage system. Journal of Energy Storage 6, 70–79.
[22] Kumaresan, G., Santosh, R., Raju, G., Velraj, R., 2018. Experimental and numerical investigation of solar flat plate cooking unit for domestic applications. Energy 157, 436–447.
[23] Hussein, H.M.S., El-Ghetany, H.H., Nada, S.A., 2008. Experimental investigation of novel indirect solar cooker with indoor PCM thermal storage and cooking unit. Energy Conversion and Management 49 (8), 2237–2246.
[24] Mussard, M., Nydal, O.J., 2013. Charging of a heat storage coupled with a low-cost small-scale solar parabolic trough for cooking purposes. Solar Energy 95, 144–154.
[25] Koçak, B., Fernandez, A.I., Paksoy, H., 2020. Review on sensible thermal energy storage for industrial solar applications and sustainability aspects. Solar Energy 209, 135–169.
[26] Li, G., 2016. Sensible heat thermal storage energy and exergy performance evaluations. Renewable and Sustainable Energy Reviews 53, 897–923.
[27] Desai, N.B., Mondejar, M.E., Haglind, F., 2022. Techno-economic analysis of two-tank and packed-bed rock thermal energy storages for foil-based concentrating solar collector driven cogeneration plants. Renewable Energy 186, 814–830.
[28] Elfeky, K.E., Mohammed, A.G., Wang, Q., 2021. Thermo-Economic Evaluation of Thermocline Thermal Energy Storage Tank for CSP Plants. Chemical engineering transactions 88.
[29] Zhou, H., Lai, Z., Cen, K., 2022. Experimental study on energy storage performances of packed bed with different solid materials. Energy 246, 123416.
[30] Cheng, Z., et al., 2014. Design and Analysis of Compact Optical Concentrators for Roof-Integrated Solar Thermal Applications. Optical Society of America.
[31] Li, Q., Zheng, C., Shirazi, A., Bany Mousa, O., Moscia, F., Scott, J.A., Taylor, R.A., 2017. Design and analysis of a medium-temperature, concentrated solar thermal collector for air-conditioning applications. Applied Energy 190, 1159–1173.
[32] Yang, M., et al., 2020. Optical and thermal performance analysis of a micro parabolic trough collector for building integration. Applied Energy 260, 114234.
[33] Lentswe, K., Mawire, A., Owusu, P., Shobo, A., 2021. A review of parabolic solar cookers with thermal energy storage. Heliyon 7 (10), e08226.
[34] SimScale (2022) Simulation Software | Engineering in the Cloud | SimScale. Available online: https://www.simscale.com/(Accessed: 4 July 2022).
[35] Domestic gas cooking appliances, in GB 16410-2020: Lingbi.
[36] Cocco, D., Serra, F., 2015. Performance comparison of two-tank direct and thermocline thermal energy storage systems for 1 MWe class concentrating solar power plants. Energy 81, 526–536.
[37] Shirazi, A., Taylor, R.A., White, S.D., Morrison, G.L., 2016. Transient simulation and parametric study of solar-assisted heating and cooling absorption systems: An energetic, economic and environmental (3E) assessment. Renewable Energy 86, 955–971.
[38] Cruickshank, C.A., Harrison, S.J., 2010. Heat loss characteristics for a typical solar domestic hot water storage. Energy and Buildings 42 (10), 1703–1710.
[39] Betti, G.T.F.S. (2021) CBE Clima Tool. Version 0.4.6. Available online: https://clima.cbe.berkeley.edu/(Accessed: 4 July 2022).
[40] Park, D., Park, E., Sunwoo, C., 2014. Heat transfer and mechanical stability analyses to determine the aspect ratio of rock caverns for thermal energy storage. Solar Energy 107, 171–181.
[41] Grirate, H., Agalit, H., Zari, N., Elmchaouri, A., Molina, S., Couturier, R., 2016. Experimental and numerical investigation of potential filler materials for thermal oil thermocline storage. Solar Energy 131, 260–274.
[42] Eastman (2022) Heat Transfer Fluids. Available online: https://www.therminol.com/heat-transfer-fluids (Accessed: 4 July 2022).
[43] Fritsch, A., Flesch, J., Geza, V., Singer, C.s., Uhlig, R., Hoffschmidt, B., 2015. Conceptual Study of Central Receiver Systems with Liquid Metals as Efficient Heat Transfer Fluids. Energy Procedia 69, 644–653.

[44] Tawfik, M.A., Sagade, A.A., Palma-Behnke, R., El-Shal, H.M., Abd Allah, W.E., 2021. Solar cooker with tracking-type bottom reflector: An experimental thermal performance evaluation of a new design. Solar Energy 220, 295–315.

[45] Fuso Nerini, F., Ray, C., Boulkaid, Y., 2016. The cost of cooking a meal. The case of Nyeri County, Kenya. Environmental research letters 12 (6), 65007.

[46] Superstore, I. (2022) Isover Spacesaver Loft Roll Insulation Glass Wool 200mm - 4.5m2 Pack | Insulation Superstore®. Available online: https://www.insulationsuperstore.co.uk/product/200mm-isover-general-purpose-loft-wool-roll-45m2.html (Accessed: 4 July 2022).

[47] Superstore, I. (2022) Isover Spacesaver Loft Roll Insulation Glass Wool 150mm - 6.99m2 Pack |. Available online: https://www.insulationsuperstore.co.uk/product/isover-spacesaver-150mm.html (Accessed: 4 July 2022).

[48] GRID, S. (2022) Electricity price. Available online: http://www.jibei.sgcc.com.cn/html/zjk/col41503/2022-03/09/20220309114429255102775_1.html (Accessed: 4 July 2022).

[49] China, T.P.B.O. (2022) Announcement on Loan Prime Rate (July 20, 2022). Available online: http://www.pbc.gov.cn/en/3688229/3688335/3883798/4611463/index.html (Accessed: 4 July 2022).

[50] IEA (2022) China – electricity generation by source. Available online: https://www.iea.org/regions/asia-pacific (Accessed: 4 July 2022).

[51] EIA (2022) How much carbon dioxide is produced per kilowatthour of U.S. electricity generation? - U.S. Energy Information Administration (EIA). Available online: https://www.eia.gov/tools/faqs/faq.php?id=74&t=11 (Accessed: 4 July 2022).

[52] Data, O.W.I. (2022) Carbon Dioxide Emissions Factor, kg CO_2 per MWh - Our World in Data. Available online: https://ourworldindata.org/grapher/carbon-dioxide-emissions-factor (Accessed: 4 July 2022).